Erbium-doped silicon-rich silicon dioxide/silicon thin films fabricated by metal vapour vacuum arc ion source implantation

2002 J. Phys.: Condens. Matter 14 L63

(http://iopscience.iop.org/0953-8984/14/3/103)

INSTITUTE OF PHYSICS PUBLISHING JOURNAL OF PHYSICS: CONDENSED MATTER

J. Phys.: Condens. Matter **14** (2002) L63–L69 PII: S0953-8984(02)31510-8

LETTER TO THE EDITOR

Erbium-doped silicon-rich silicon dioxide/silicon thin films fabricated by metal vapour vacuum arc ion source implantation

Fei Xu[1], Zhisong Xiao[2], Guoan Cheng[3], Zhongzhen Yi[3], Tonghe Zhang[3], Lanlan Gu[1] and Xun Wang[1,4]

[1] Surface Physics Laboratory, Fudan University, Shanghai 200433, China
[2] Department of Electronic Engineering, The Chinese University of Hong Kong, Shatin, NT, Hong Kong, China
[3] Laboratory for Radiation Beam and Material Modification, Institute of Low Energy Nuclear Physics, Beijing Normal University, Beijing 100875, China

E-mail: xunwang@fudan.ac.cn

Received 20 July 2001
Published 8 January 2002
Online at stacks.iop.org/JPhysCM/14/L63

Abstract

A new method, metal vapour vacuum arc ion source implantation, has been developed to synthesize Er-doped Si-rich SiO_x thin films under relatively low implanted ion energies and very high doses. An Er concentration as high as $\sim 10^{21}$ atoms cm^{-3} in the Si oxide layer can be reached. Reflection high-energy electron diffraction and cross section transmission electron microscopic observations show that the excess Si atoms in the SiO_2 matrix cluster and crystallize gradually into nano-size grains with an average size of 4.5 nm during the rapid thermal annealing process after dual-implantation. The sample emits a 1.54 μm wavelength luminescence signal, the intensity of which decreases by only a factor of two as the measuring temperature increases from 77 K to 300 K, showing very weak temperature quenching.

1. Introduction

The investigation of Er doping in Si has become an interesting topic since Ennen *et al* observed 1.54 μm light emission in Er-doped silicon at 20 K in 1983 and later obtained electroluminescence at 77 K in 1985 [1, 2]. If achieved, efficient light emission from Si-based luminescent thin film will perhaps lead to a new era of Si-based optoelectronic integration [3–5]. It has been found that the 1.54 μm light emission of Er-doped Si usually shows very strong temperature dependence. The strong photoluminescence (PL) intensity observed at low temperature will decrease by several orders of magnitude when the temperature rises to 300 K.

[4] Corresponding author.

This temperature quenching is believed to be caused by energy back transfer in the de-excitation process. One method to avoid temperature quenching is to incorporate Er into wide bandgap Si-based host materials, such as SiO_2 and Si-rich SiO_x oxide layers. Many approaches have been developed to manufacture these silicon oxides, amongst which ion implantation is the most popular.

Metal vapour vacuum arc (MEVVA) ion source implantation [6, 7] is a newly developed method that can produce strong-flux high-dose ion beams to modify material surfaces. It has been widely used in industry to improve material properties such as surface hardness, wear resistance, corrosion resistance, fatigue resistance, etc [8–10]. In this work we employ MEVVA ion source implantation to prepare Er-doped Si-rich Si oxide thin films. The Er concentration in oxide films can reach to $\sim 10^{21}$ cm^{-3}, which is much higher than the Er concentrations obtained in Si or SiO_2 by other techniques, for example, ordinary high-energy ion implantation. The near infrared (IR) PL shows very weak temperature quenching, with the 1.54 μm PL peak intensity reduced only by a factor of two when the temperature changes from 77 K to 300 K.

2. Experimental details

The substrates used were Czochralski grown p-type (100)-oriented Si single crystal wafers with a resistivity of 3–5 Ωcm. First, thin SiO_2 film was grown on Si substrates by thermal oxidation under a high-pressure stream ambient of 5N O_2 gases in a high-temperature diffusion furnace. The oxidation temperature was 820 °C. The thickness of the SiO_2 film was 90 nm, as determined by ellipsometry, which was thick enough to meet the requirement that the subsequently implanted Si and Er atoms remain within the Si oxide layer. Then Si and Er ions were dual-implanted into the thermal SiO_2/Si thin films using a MEVVA ion implanter, both with accelerating voltages of 45 kV. The Si and Er ion flux densities were 85 and 5 μA cm^{-2}, and the doses 5×10^{17} and 1×10^{17} ions cm^{-2}, respectively. A Monte Carlo simulation with the program TRIM'96 was used to design the depth profiles of the implanted Si and Er ions. After dual-implantation, the samples were treated by rapid thermal annealing (RTA) at 1000 °C for 20 s under ambient argon gas.

The characterization of the (Si, Er) dual-implanted SiO_2/Si thin films was carried out by Rutherford backscattering (RBS), x-ray photoelectron spectroscopy (XPS), reflection high-energy electron diffraction (RHEED), high-resolution transmission electron microscopy (HRTEM), and photoluminescence. The energy of the He^+ ion beam in RBS was 2 MeV. The backscattered ions were detected by an Au/Si surface barrier detector placed at a scattering angle of 165°. The XPS x-ray source used Mg K_α radiation with a photon energy of 1253.6 eV and an energy resolution of about 0.68 eV. The RHEED observations were performed using a JEM-200CX analytical transmission electron microscope with an accelerating voltage of 160 kV. The cross section of the sample was characterized by a Hitachi H-9000 high-resolution transmission electron microscope with a resolution of 0.18 nm. The PL spectra were measured in the near-IR range around 1.54 μm under the excitation of a 30 mW He–Cd laser pump at 441.6 nm. The signals were focused by two lenses, collected by a monochromator and detected by a liquid nitrogen cooled Ge detector. The sample temperatures in the PL measurements were 77 and 300 K.

3. Results and discussion

First, the compositions of the (Si, Er) dual-implanted Si oxide layers were determined by RBS and XPS. Figure 1 shows the typical RBS spectrum of the annealed sample with a nominal SiO_2 thickness of 90 nm. The arrows in the figure indicate RBS energies corresponding to Er, Si and O located at the sample surface. The plateau of the RBS signal around 1.08 MeV is attributed to the signal of Si from the silicon oxide layer. It is calculated by the stopping cross section factor method that the energy width of the Si plateau $\Delta E_{\mathrm{Si}} \equiv 37.2$ keV corresponds to a thickness of $\sim$72 nm. This is a little smaller than the nominal thickness of the thermal SiO_2. The decrease of the oxide thickness is believed to be caused by the sputtering effect during Si and Er dual-implantation. Figure 2 shows the Si and Er concentration depth profiles derived from the RBS spectrum by the known stopping powers. The Er concentration depth profile is different from the Gaussian function that describes the approximate depth distribution in the sample prepared by high-energy ion implantation. It is a result of the relatively low ion energies and very high doses in our case. The Er peak concentration is about 9.2 at.% at a depth of 30 nm. The Er concentration is basically distributed in the Si oxide layer. It can be roughly estimated that the average excess Si content in the Si oxide layer is $\sim$20.7 at.% and the average Er content about 6.7 at.%. These results agree well with the data simulated by the TRIM'96 program. Figure 3 shows the XPS spectra of Si2p, Er4d and O1s for the sample after RTA at 1000 °C for 20 s. The ratio of the Er, Si and O concentrations on the surface are calculated by the atomic sensitivity factor method. In figure 3(*a*), the dashed curves under the Si2p peak are fitted with Gaussian functions. The peak at 100.7 eV with a full width at half maximum (FWHM) of 1.7 eV is from Si, while the other at 103.9 eV with a FWHM of 2.6 eV is from SiO_2. From the areas of these two peaks, we can estimate that there are about 11.1 and 23.2 at.% Si atoms in the pure Si and SiO_2 states, respectively. The O1s binding energy is 532.8 eV with a FWHM of 2.9 eV. This value is the O1s binding energy of SiO_2. The Er concentration in the surface of the annealed sample

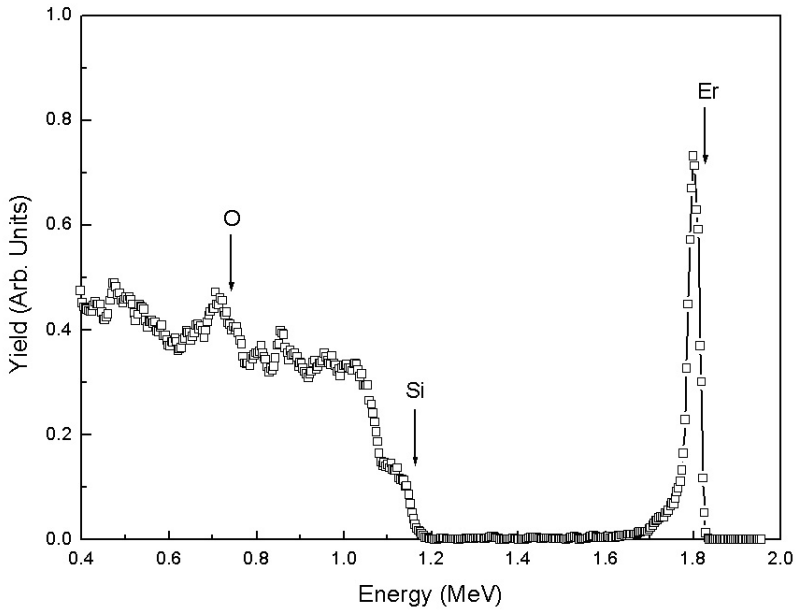

Figure 1. Typical RBS spectrum of the annealed sample with a nominal SiO_2 thickness of 90 nm.

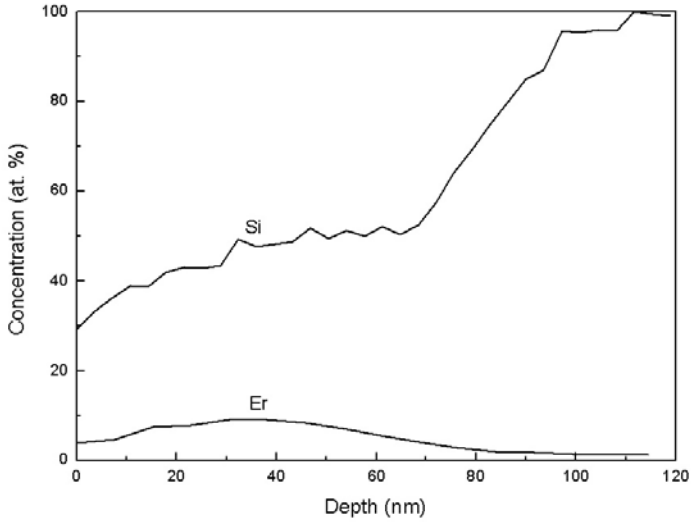

Figure 2. Si and Er concentration depth profiles derived from figure 1.

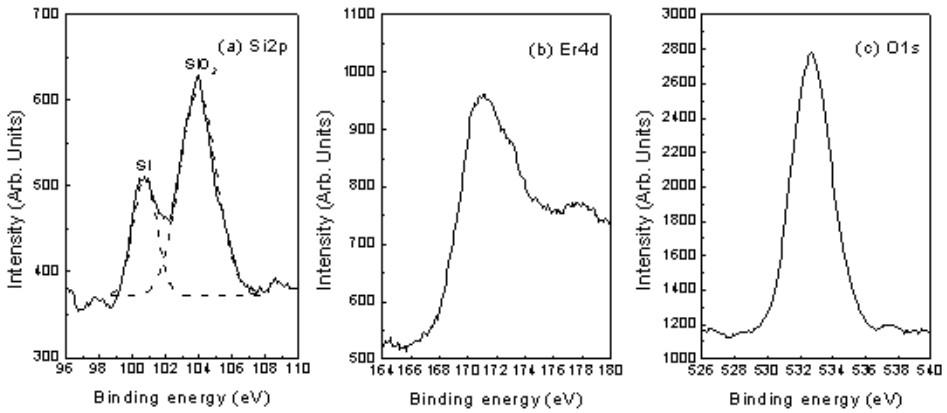

Figure 3. XPS spectra of Si2p, Er4d and O1s for the sample after RTA at 1000 °C for 20 s.

is estimated to be 4.4 at.% corresponding to a bulk concentration of 2.2×10^{21} cm^{-3}. This is almost consistent with the Er concentration in the surface of the Si oxide layer analysed by RBS. We notice that the Er peak shape is different from that of erbium silicide and the Si2p peak from erbium silicide is not present, so we can conjecture that Er atoms located in the Si oxide layer exist in the form of isolated Er atoms or as Er_2O_3. Therefore, the incorporation of Er in the SiO_2 layer by a MEVVA ion source would be a better way to achieve higher Er concentration than other methods, for example high-energy ion implantation and molecule beam epitaxy.

Figure 4 shows RHEED patterns from the surface of the sample before and after RTA. For the as-implanted sample, a diffused diffraction disc is observed (figure 4(a)). After RTA, well-distributed diffraction circles of Si polycrystals are visible, as shown in figure 4(b), suggesting that Si clusters are re-crystallized into Si crystalline particles such as Si nanocrystals (nc-Si).

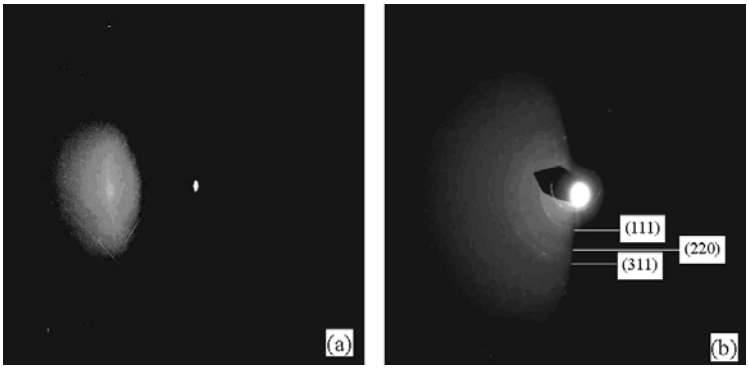

Figure 4. RHEED patterns from the surface of the sample before (a) and after (b) RTA.

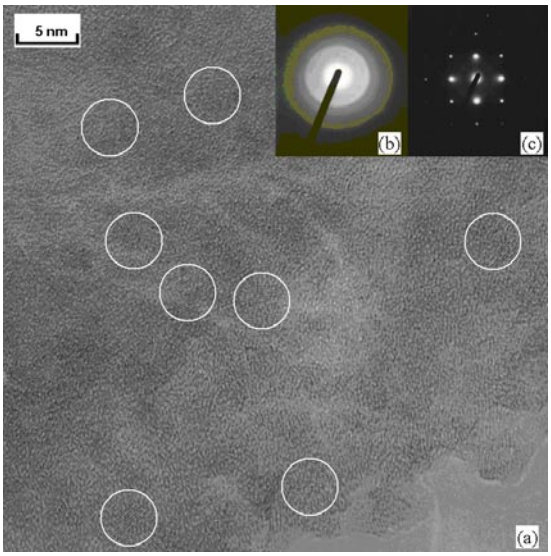

Figure 5. Cross-sectional HRTEM and electron diffraction patterns of the annealed sample.

From the absence of Er diffraction circles or spots on the surface of the annealed sample, we postulate that Er segregation and the formation of precipitates such as $ErSi_2$, $ErSi_{2-x}$ or Er_2Si_5 seem unlikely. To check the existence of nc-Si in the SiO_2 matrix, cross-section TEM observation was carried out, as shown in figure 5. In figure 5(a), the HRTEM image shows that nc-Si is identifiable in the regions marked with circles. The electron diffraction patterns taken from these areas show well-distributed diffraction circles of Si polycrystals (figure 5(b)) and diffraction spots of Si single crystals (figure 5(c)). It is estimated that the sizes of nc-Si with good crystallinity range from 2–6 nm in diameter and their average size is ∼4.5 nm. The diffraction pattern of nc-Si corresponds to the {100} plane of Si. Diffraction circles or spots of Er segregation or Er precipitates are not found. We postulate that Si ions introduced by ion implantation accumulated to form Si clusters, and then Si crystal particles such as nc-Si formed during RTA.

Figure 6 shows the near-IR PL around 1.54 μm for the annealed sample measured at 77 K and 300 K. There is no 1.54 μm light signal observed in the as-implanted sample. The PL

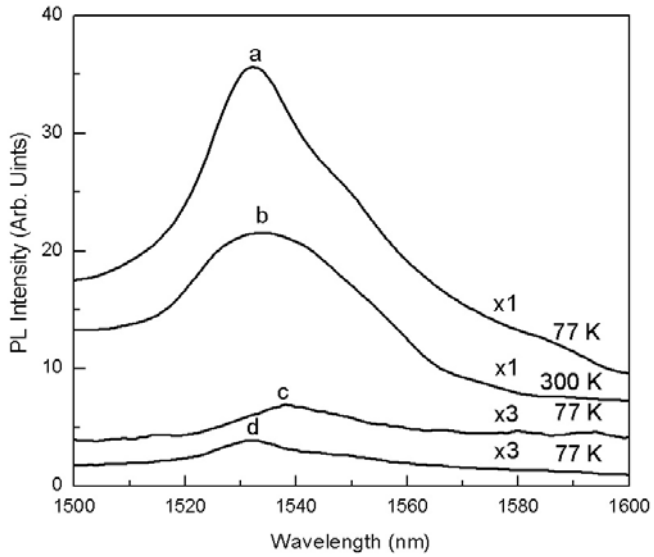

Figure 6. Near-IR PL spectra of (a) Si and Er dual-implanted SiO_2 at 77 K, (b) Si and Er dual-implanted SiO_2 at 300 K, (c) Si and Er dual-implanted c-Si at 77 K and (d) Er-implanted SiO_2 at 77 K.

around 1.54 μm has a main peak at 1532 nm with a FWHM of 35 nm at 77 K. The FWHM at 300 K is 42 nm, which is a little broader than that at 77 K. The integrated intensity decreases by less than 50% when the measuring temperature changes from 77 to 300 K. This indicates that the temperature quenching of our sample is not so serious, possibly because of the formation of nc-Si in the Si oxide layer which reduces the non-radiative de-excitation processes. To make a comparison, curves (c) and (d) in figure 6 give the PL spectra of two samples. One is formed by Si and Er dual-implantation in the Si substrate, and the other by Er single-implantation in the SiO_2/Si film. The intensities of the 1.54 μm light emission signals from these two samples are only 1/30 that of the Si-plus-Er dual-implanted SiO_2/Si thin film at 77 K. The PL spectra are not visible in these two samples at 300 K.

The above PL spectra verify that both the replacement of host material Si by SiO_2 and the formation of nano-crystalline Si in the SiO_2 matrix play the main roles in improving the luminescence behaviour. However, to clarify the exact mechanism of this improvement, further investigation is necessary.

4. Conclusion

Si and Er dual-implanted thermal SiO_2/Si luminescent thin film has been synthesized by MEVVA ion source implantation. Very high Er concentration in Si-rich SiO_2 could be obtained, reaching an order of 10^{21} cm^{-3}. The average excess Si content in the Si oxide layer is $\sim$20.7 at.%. The Si clusters are gradually crystallized into nc-Si by rapid thermal annealing. The diameters of the nc-Si particles with a good crystallinity range from 2–6 nm, with an average value of $\sim$4.5 nm. Near-IR PL spectra around 1.54 μm could be observed at 77 and 300 K after the sample was annealed at 1000 $^\circ$C for 10 s. Very weak temperature quenching is achieved, which may be attributed to the formation of nc-Si in the Si oxide layer, which then reduces the non-radiative de-excitation processes.

This work was supported partially by the National Natural Science Foundation of China Grant No 6976601, and the 863 High Technology Committee of China. The authors are grateful to Professor Honglie Shen and Mr Pan Qiang at the Shanghai Institute of Metallurgy, Chinese Academy of Sciences for the measurements. We thank also Professor Zhenglong Wu from the Analytic Testing Center in Beijing Normal University for the XPS measurements.

References

[1] Ennen H, Schneider J, Pomrenke G and Axmann A 1983 *Appl. Phys. Lett.* **43** 943
[2] Ennen H, Pomrenke G, Axmann A, Eisele K, Haydl W and Schneider J 1985 *Appl. Phys. Lett.* **46** 381
[3] Benton J L, Michel J, Kimerling L C, Jacobson D C, Xie W H, Eaglesham D J, Fitzgerald E A and Poate J M 1991 *J. Appl. Phys.* **70** 2667
[4] Priolo F, Coffa S, Franzo G, Spinella C, Carnera A and Bellani V 1993 *J. Appl. Phys.* **74** 4936
[5] Wan J, Sheng C, Lu F, Yuan S, Gong D W, Liao L S, Fang Y L and Wang X 1999 *J. Lumin.* **80** 367
[6] Brown I G, Feinberg B and Galivin J E 1988 *J. Appl. Phys.* **63** 4889
[7] Zhang H X, Zhang X J, Zhou F S, Li Q, Wu X Y, Lin W L and Zhang T H 1998 *Surf. Coat. Tech.* **103–104** 280
[8] Zhang T H, Wang X Y, Liang H, Zhang H X, Zhou G, Sun G R, Zhao W J and Xue J M 1996 *Surf. Coat. Technol.* **83** 280
[9] Cheng G A, Xiao Z S, Zhu J H, Xu S L and Ye D R 1998 *Nucl. Instrum. Methods* B **135** 550
[10] Zhang T H, Ji C Z, Xie J D, Chen J, Wei F Z, Sun G R and Gao Y Z 1994 *Vacuum* **45** 945